Developmental Cell
Article

A Ras Signaling Complex Controls the RasC-TORC2 Pathway and Directed Cell Migration

Pascale G. Charest,[1] Zhouxin Shen,[1] Ashley Lakoduk,[1] Atsuo T. Sasaki,[1,2] Steven P. Briggs,[1] and Richard A. Firtel[1,*]
[1]Section of Cell and Developmental Biology, Division of Biological Sciences, University of California, San Diego, 9500 Gilman Drive, La Jolla, CA 92093-0380, USA
[2]Present address: Department of Systems Biology, Harvard Medical School, Division of Signal Transduction, Beth Israel Deaconess Medical Center, 77 Avenue Louis Pasteur, Boston, MA 02115, USA
*Correspondence: rafirtel@ucsd.edu
DOI 10.1016/j.devcel.2010.03.017

SUMMARY

Ras was found to regulate *Dictyostelium* chemotaxis, but the mechanisms that spatially and temporally control Ras activity during chemotaxis remain largely unknown. We report the discovery of a Ras signaling complex that includes the Ras guanine exchange factor (RasGEF) Aimless, RasGEFH, protein phosphatase 2A (PP2A), and a scaffold designated Sca1. The Sca1/RasGEF/PP2A complex is recruited to the plasma membrane in a chemoattractant- and F-actin-dependent manner and is enriched at the leading edge of chemotaxing cells where it regulates F-actin dynamics and signal relay by controlling the activation of RasC and the downstream target of rapamycin complex 2 (TORC2)-Akt/protein kinase B (PKB) pathway. In addition, PKB and PKB-related PKBR1 phosphorylate Sca1 and regulate the membrane localization of the Sca1/RasGEF/PP2A complex, and thereby RasC activity, in a negative feedback fashion. Thus, our study uncovered a molecular mechanism whereby RasC activity and the spatiotemporal activation of TORC2 are tightly controlled at the leading edge of chemotaxing cells.

INTRODUCTION

Chemotaxis, the guided movement of cells in response to external cues or chemoattractants, is central to numerous biological processes, including embryogenesis, the immune response, and metastasis of tumor cells. Chemotaxis is equally central to the life cycle of *Dictyostelium*, allowing the free-living amoebae to chase bacteria, their food source, as well as to aggregate and form multicellular structures upon starvation (Annesley and Fisher, 2009). Aggregation of *Dictyostelium* cells is driven by their ability to respond to the chemoattractant cAMP and to relay the signal through chemoattractant-induced activation of adenylyl cyclase A (ACA) and the subsequent secretion of cAMP in an oscillatory fashion (signal relay).

Studies over the past few years have uncovered key signaling pathways involved in the chemotactic response of amoeboid cells, such as *Dictyostelium* and neutrophils, and have shed light on the spatial and temporal regulation of these pathways, which is required for cells to perform efficient chemotaxis. Ras proteins play major roles in the control of *Dictyostelium* chemotaxis. Ras activation is the earliest known response to chemoattractant stimulation downstream from the receptors and heterotrimeric G proteins, and active Ras is enriched at the leading edge of chemotaxing cells (Sasaki et al., 2004). Two *Dictyostelium* homologs of human H-Ras, RasC and RasG, control cell motility, chemotaxis, and signal relay, acting in part through the regulation of phosphatidyl-inositol 3-kinase (PI3K) and target of rapamycin complex 2 (TORC2), two known regulators of Akt/protein kinase B (PKB) (Bolourani et al., 2006; Funamoto et al., 2002; Kamimura et al., 2008; Lee et al., 1999, 2005; Lim et al., 2001; Meili et al., 1999; Sasaki and Firtel, 2006; Sasaki et al., 2007). The recent findings that Ras is an important regulator of PI3Kγ signaling in migrating neutrophils and that human Sin1, a component of mammalian TORC2 and the ortholog of *Dictyostelium* Ras interacting protein 3 (RIP3), binds activated H- and K-Ras suggest that the role of Ras in directed cell migration may be conserved in mammalian cells (Schroder et al., 2007; Suire et al., 2006). In *Dictyostelium*, the site of Ras activation directly determines the site of PI3K activation and PI(3,4,5)P_3 production, which then helps guide the local polymerization of F-actin and pseudopod extension (Affolter and Weijer, 2005; Huang et al., 2003; Para et al., 2009; Sasaki et al., 2004; Zhang et al., 2008). TORC2 is also an important regulator of *Dictyostelium* chemotaxis, controlling cell polarity and motility, as well as signal relay, through regulation of the cytoskeleton and ACA activity, respectively (Kamimura et al., 2008; Lee et al., 2005). In addition, recent observations suggest that TORC2 activity is spatially regulated at the leading edge of migrating cells, causing the local activation of PKB and PKB-related PKBR1 (Kamimura et al., 2008). While RasC and RasG appear to be partially redundant, evidence suggests that signal transduction through RasC is more important for ACA activation, whereas RasG plays a more important role in PI3K activation; and disruption of both RasC and RasG signaling results in cells that exhibit severe polarity and directional sensing defects (Bolourani et al., 2006; Sasaki et al., 2004; Zhang et al., 2008).

Several years ago, a *Dictyostelium* homolog of the mammalian Ras guanine exchange factor (RasGEF) SOS, Aimless/RasGEFA, was found to play an important role in the transduction of chemotactic signals (Insall et al., 1996; Lee et al., 1999). Subsequent studies suggest that Aimless is the major RasGEF mediating the chemoattractant-induced activation of RasC,

whereas other RasGEFs, including RasGEFR, activate RasG (Kae et al., 2007). The present study was undertaken to identify regulators of Ras signaling during *Dictyostelium* chemotaxis and to better understand the mechanisms implicated in the spatiotemporal control of Ras activity. Using a proteomic approach, we identified a multimeric protein complex that includes Aimless, RasGEFH, PHR, and protein phosphatase 2A (PP2A), assembled by the scaffold protein Sca1. We demonstrate that this Ras signaling complex regulates the RasC-TORC2-Akt/PKB pathway at the leading edge of chemotaxing cells and undergoes TORC2- and Akt/PKB-dependent negative feedback regulation.

RESULTS

Aimless Is Part of a Stable Protein Complex

To study the molecular mechanisms that regulate Ras signaling during chemotaxis, we took a proteomic approach to identify proteins interacting with the RasGEF Aimless. We expressed His/HA/FLAG (HHF)-tagged Aimless in *gefA*$^-$ (*aimless* null, *aleA*$^-$) cells and performed a sequential FLAG-His affinity purification. Several proteins copurified with Aimless in both vegetative and developed cells and the profile of the pulled down proteins did not change upon cAMP stimulation of developed cells, suggesting their interaction with Aimless is not modulated by chemoattractant stimulation (Figure 1A). Mass spectrometry analysis allowed identification of the Aimless-interacting proteins: another RasGEF, RasGEFH; the structural A subunit of PP2A (PP2A-A, gene: *pppA*) and a putative catalytic C subunit we named PP2A-C2 (gene: *pho2B*); an uncharacterized 174.9 kDa protein we named Sca1; and a 111.6 kDa protein that contains a pleckstrin homology domain as well as a Ras GTPase-related domain we named PHR (Figure 1A; see Table S1 available online). Although these proteins were found to be the most abundant, additional proteins were identified in the Aimless pull-down, most of which are proteins associated with the protein synthesis, folding, or degradation machineries and thus are less likely to represent interactions required for RasGEF function (Table S1). Aimless and RasGEFH are very similar and both display a Lissencephaly 1 (Lis1) homology motif (LisH), a putative dimerization domain (Gerlitz et al., 2005; Mateja et al., 2006). PP2A-A and -C2 most likely form a core PP2A dimer as PP2A holoenzymes typically contain a structural A and a catalytic C subunit, constituting an enzymatic core dimer that associates with a third, variable regulatory B subunit (Janssens et al., 2008). Interestingly, the gene encoding Sca1 (*scaA*) was identified previously in a screen for developmentally essential genes required for aggregation (*DG1105*; dictyBase).

To assess whether Aimless interacts with each of the pulled down proteins independently or if the proteins are in a large multimeric complex, we analyzed and compared pull-downs performed with individually epitope-tagged Aimless, RasGEFH, or Sca1, each expressed in their respective null background. As shown in Figure 1B and Figure S1A, all three proteins pull down each other, as well as PHR and PP2A-A/C2, suggesting Aimless, RasGEFH, Sca1, PHR, and PP2A-A/C2 form a single, stable protein complex. RasGEFH and PHR are absent from a pull-down performed with Aimless when Aimless' LisH domain is mutated (Aimless^{LisH-}; two conserved residues found to stabilize LisH domain homodimerization in human Lis1), suggesting that the presence of these two proteins in the complex requires interaction with Aimless' LisH domain (Figure 1B; Figure S1A).

To confirm the pull-down data and better understand the structure of the complex, we assessed the interaction between the different components by coimmunoprecipitation. As shown in Figures 1C and 1D, Aimless and RasGEFH coimmunoprecipitate each other, even in the absence of Sca1, but mutation of the LisH domain in either one of the RasGEFs prevents their copurification. In contrast, we never observed any coimmunoprecipitation of two differentially tagged RasGEFHs or two differentially tagged Aimless proteins (Figure 1E). These findings suggest that Aimless and RasGEFH directly interact through their LisH domain, forming an exclusive heterodimer. Because Aimless and RasGEFH appear to directly interact through their LisH domain, and an Aimless^{LisH-} mutant fails to pull down PHR in addition to RasGEFH, we suggest PHR interacts directly with RasGEFH.

We then tested the interaction of Sca1 with the RasGEFs and PP2A. As shown in Figure 1F, Aimless and Sca1 coimmunoprecipitate each other, independently of Aimless' LisH domain and RasGEFH. In addition, although RasGEFH and Sca1 were found to coimmunoprecipitate, they did not do so in the absence of Aimless, consistent with the interaction between RasGEFH and Sca1 being indirect, most likely through Aimless (Figure 1G). Finally, we determined that Sca1 and PP2A-A coimmunoprecipitate each other, even in the absence of both RasGEFs (Figure 1H). To further investigate the molecular architecture of the complex, we generated a series of Sca1 deletion mutants and assessed their interaction with the other components in pull-down assays (Figure 1I). As shown in Figure 1J and Figure S1B, deletion of residues 401–600 (Sca1Δ2) results in the complete loss of interaction of the RasGEFs, but not PP2A, with Sca1, whereas mutants with deletions between residues 600 and 1400 (Sca1Δ3–Δ6) affect the interaction of Sca1 with PP2A. Although some PP2A was detected in pull-downs with Sca1Δ3 and Δ4, Sca1Δ5 and Δ6 appear to completely lose interaction with PP2A, while interaction with the RasGEFs is normal. Altogether, these findings suggest that Sca1 acts as a molecular scaffold, bringing together the RasGEFs and PHR with PP2A (Figure 1K).

The Sca1 Complex Regulates Cell Motility, Chemotaxis, and Signal Relay

To determine the biological function of the Sca1 complex, we analyzed the phenotypes of mutant strains in which the different components of the complex were disrupted either alone or in combination. As shown in Figure 2A and Figure S2A, the analysis of the developmental phenotypes of cells lacking PHR, RasGEFH, Aimless, or Sca1 reveals that whereas the development of *phr*$^-$ and *gefH*$^-$ cells is slightly delayed compared to that of wild-type cells, cells lacking Aimless, both RasGEFs, or Sca1 display severely impaired aggregation. Interestingly, although expression of full-length Sca1 complements the *scaA*$^-$ cells' developmental phenotype, expression of the Sca1Δ2 deletion mutant, which fails to interact with the RasGEFs, the mutants that most severely disrupt the interaction

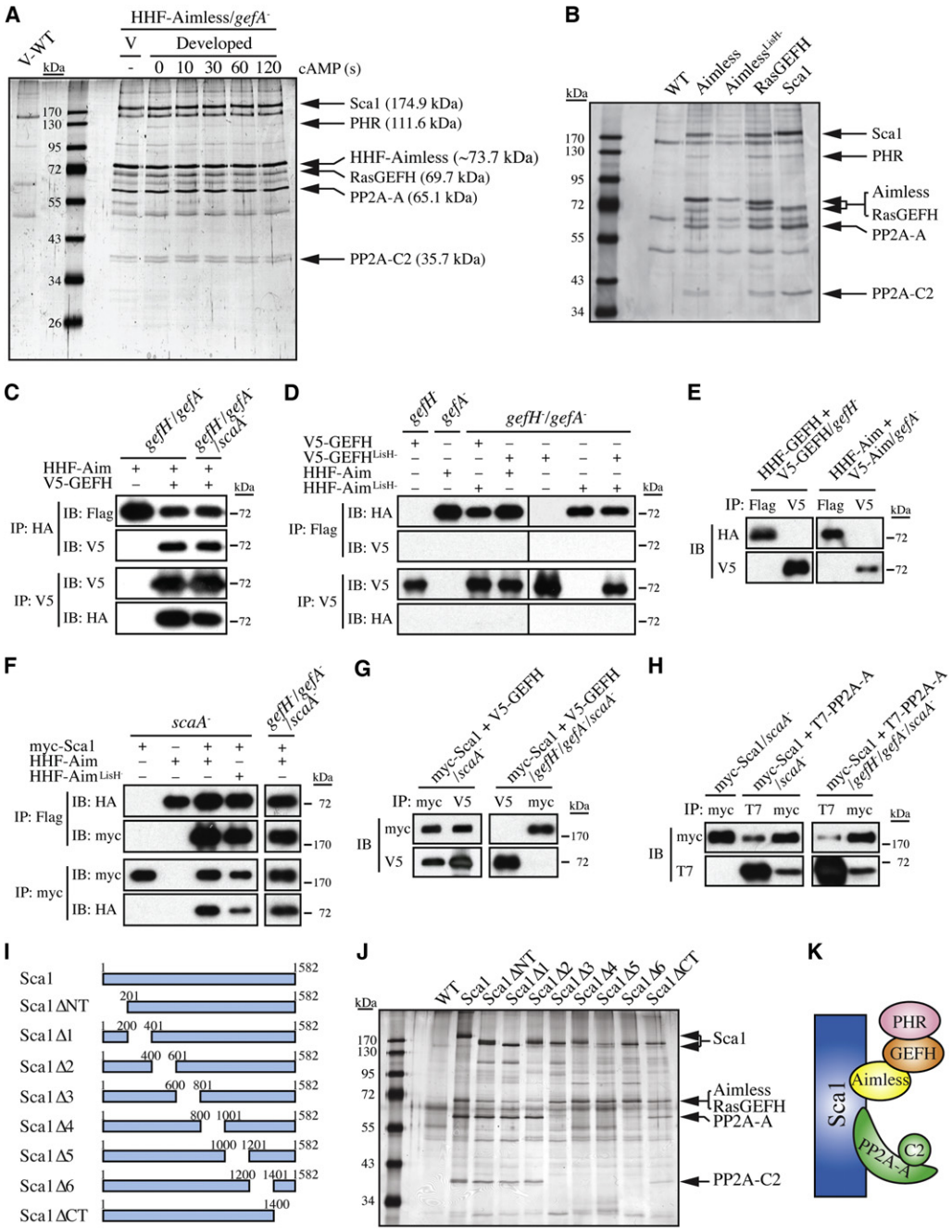

Figure 1. Aimless Is Found in a Preformed Complex Assembled by the Scaffold Protein Sca1

(A and B) Silver staining of the SDS-PAGE-resolved proteins pulled down with HHF-Aimless, -Aimless^{LisH}, -RasGEFH, or -Sca1, expressed in their respective null background, from either vegetative (V) or developed cells stimulated or not with 1 μM cAMP for the time indicated. Wild-type cells (WT; AX2) were used as controls. The most abundant purified proteins identified by mass spectrometry and their molecular mass are indicated. Aimless (70.7 kDa) and RasGEFH (69.7 kDa) normally migrate at a similar molecular mass; addition of the HHF tag underlies the observable shifts (HHF-Aimless, ~73.7 kDa; HHF-RasGEFH, ~72.7 kDa). See also Table S1 and Figure S1A.

(C–H) HHF- or V5-tagged Aimless (HHF-Aim and V5-Aim) and RasGEFH (HHF-GEFH and V5-GEFH), their LisH domain mutant forms [Aim^{LisH-}, Aimless (L79E, E94A); GEFH^{LisH-}, RasGEFH (F127R, E142A)], and myc-Sca1 and T7-PP2A-A were assessed for interaction in coimmunoprecipitation (IP) and detected by immunoblotting (IB).

(I) Sca1 deletion mutants.

(J) Pull-downs performed with the Sca1 deletion mutants compared to full-length Sca1. See also Figure S1B.

(K) Deduced architecture of the complex. Data are representative of at least two independent experiments.

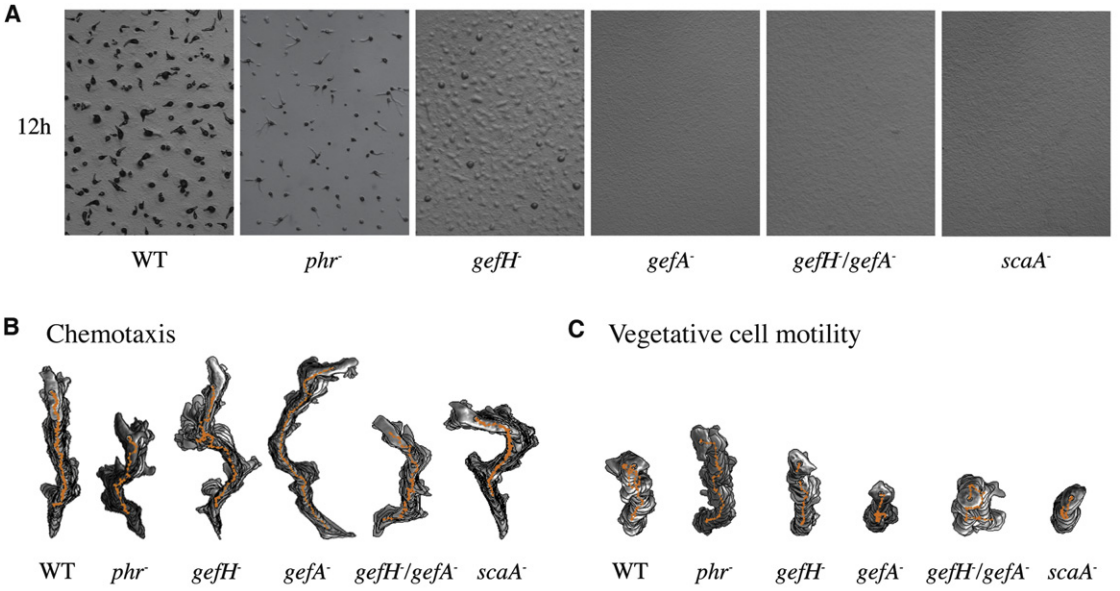

Strain	Speed (μm/min)	Directionality	Direction change (deg)	Roundness (%)
AX2	8.1 ± 2.7	0.86 ± 0.04	33 ± 9	35 ± 5
phr⁻	6.9 ± 1.5	0.65 ± 0.12	35 ± 9	35 ± 6
gefH⁻	9.4 ± 1.1	0.75 ± 0.10	36 ± 9	31 ± 7
gefA⁻	11.7 ± 2.5	0.78 ± 0.09	24 ± 8	32 ± 4
gefH⁻/*gefA*	6.6 ± 0.7	0.53 ± 0.03	40 ± 2	41 ± 4
scaA⁻	8.0 ± 1.0	0.63 ± 0.08	39 ± 6	27 ± 2

Strain	Speed (μm/min)	Persistence	Direction change (deg)	Roundness (%)
AX2	3.8 ± 1.3	0.43 ± 0.13	39 ± 7	59 ± 7
phr⁻	5.9 ± 1.3	0.77 ± 0.24	26 ± 3	50 ± 4
gefH⁻	3.2 ± 1.3	0.46 ± 0.30	36 ± 7	62 ± 6
gefA⁻	2.6 ± 1.7	0.27 ± 0.26	54 ± 17	61 ± 9
gefH⁻/*gefA*	2.5 ± 1.1	0.29 ± 0.15	44 ± 11	69 ± 6
scaA⁻	1.6 ± 0.7	0.15 ± 0.10	55 ± 9	69 ± 5

Figure 2. The Sca1 Complex Regulates Aggregation, Chemotaxis, and Vegetative Cell Motility

(A) Development of the different knockout strains compared to wild-type. Shown pictures were taken at 12 hr after starvation. Data are representative of three independent experiments. See also Figure S2.

(B and C) DIAS analysis and traces of representative developed cells performing chemotaxis to cAMP (B) or randomly moving vegetative cells (C). Data represent analysis performed on ten traces from three independent experiments ± SD. Speed refers to the speed of the cell's centroid movement along the total path; directionality indicates migration straightness; persistence indicates the persistence of movement in a given direction; direction change refers to the number and frequency of turns; and roundness indicates cell polarity.

with PP2A (Sca1Δ4–Δ6), as well as Sca1ΔCT, fail to complement the *scaA*⁻ cell phenotype (Figure S2B). Unfortunately, efforts to disrupt *pppA* and *pho2B* were unsuccessful. As another group also reported unsuccessful attempts to disrupt *pppA*, we suggest that PP2A is essential for growth (Murphy et al., 1999).

The subsequent analysis of developed, single cells revealed that *phr*⁻, *gefH*⁻, *gefA*⁻, *scaA*⁻, and *gefH*⁻/*gefA*⁻ display directionality defects during chemotaxis (Figure 2B; Movie S1). In addition, we found that vegetative *gefA*⁻, *gefH*⁻/*gefA*⁻, and *scaA*⁻ cells all display defects in random motility (absence of chemoattractant), as indicated by their reduced speed and persistence of movement compared to wild-type cells (Figure 2C). Intriguingly, we observed that vegetative *phr*⁻ cells move considerably faster and with greater persistence than wild-type cells. These observations suggest that the Sca1 complex regulates cell motility, chemotaxis, and also, presumably, signal relay during aggregation, as cells lacking Aimless or Sca1 do not stream (data not shown).

Since the loss of RasGEFH in the complex entails the loss of PHR and *phr*⁻ cells display phenotypes distinct from those of the other Sca1 complex null cells, it appears that PHR might play a different role in the regulation of chemotaxis than the other components of the Sca1 complex (see Discussion). Therefore, we did not include further analysis of PHR in the present study.

The Sca1 Complex Controls RasC Signaling at the Leading Edge

To investigate the function of the Sca1 complex, we first assessed the chemoattractant-mediated activation of Ras in the different Sca1 complex null backgrounds. In Figure 3A and Figure S3A, we show that the Sca1 complex regulates RasC activity while RasG activation is unaffected. Chemoattractant-induced activation of RasC is reduced in *gefH*⁻ cells and is almost completely absent in *gefA*⁻ cells, whereas cells lacking the two RasGEFs or Sca1 totally fail to induce RasC activation, indicating Aimless and RasGEFH are required for RasC activation. In addition, we found that PKB activity is gradually reduced in the different null strains, with the strongest reduction observed in *scaA*⁻, and F-actin polymerization is also reduced (Figures 3B and 3C). Interestingly, we found that chemoattractant-induced accumulation of cAMP is reduced in *gefH*⁻ cells and absent in *gefA*⁻, *gefH*⁻/*gefA*⁻, and *scaA*⁻, in a way that correlates with the level of RasC activity in each strain (Figure 3D). In addition, we determined that *pkb*⁻/*pkbr1*⁻ cells completely fail to stimulate cAMP accumulation in response to chemoattractant stimulation, suggesting that the two kinases might be downstream from RasC in the pathway leading to ACA activation. Therefore, impaired signaling to the actin cytoskeleton and ACA most likely underlies the aggregation, cell motility, and chemotaxis defects of the Sca1 complex null mutants. Interestingly, we also found

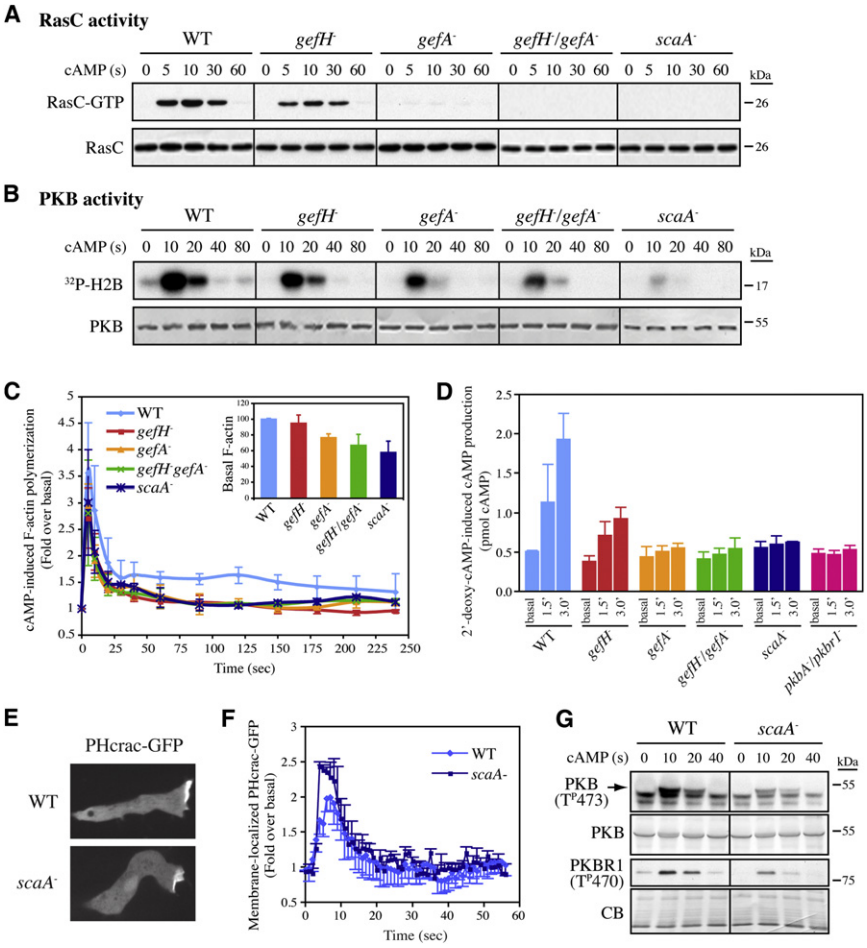

Figure 3. The Sca1 Complex Controls the RasC-TORC2-PKB/PKBR1 Pathway

(A) FLAG-RasC was expressed in the indicated strains and cAMP-induced RasC activity was assessed following pull-down of active RasC (RasC-GTP) with GST-RBD(Byr2). Pulled down and total RasC were revealed by FLAG immunoblotting. See also Figure S3.

(B) cAMP-induced kinase activity of immunoprecipitated PKB was assessed using H2B as a substrate. H2B phosphorylation was detected by autoradiography and PKB was revealed by immunoblotting.

(C) Basal (inset; expressed as percentage of wild-type) and cAMP-induced F-actin polymerization.

(D) Total cAMP production in response to stimulation by 10 μM 2′-deoxy-cAMP for the time indicated.

(E) Imaging of PHcrac-GFP in wild-type and *scaA*$^-$ performing chemotaxis to cAMP.

(F) Translocation of PHcrac-GFP to the plasma membrane upon uniform cAMP stimulation. The graph depicts the relative fluorescence intensity of membrane-localized PHcrac-GFP as a function of time after cAMP stimulation. Data represent the measured membrane fluorescence intensity of ten different cells.

(G) cAMP-induced phosphorylation of immunoprecipitated PKB at threonine 473 (T^P473) and of PKBR1 from total cell lysates at threonine 470 (T^P470). Immunoprecipitated PKB was revealed by immunoblotting, and Coomassie blue (CB) staining was used as loading control for total cell lysates. Data are representative or represent the mean ± SD (C and D) or SEM (F) of at least three independent experiments.

that activation of RasC induced by the chemoattractant folate in vegetative cells is greatly reduced in *scaA*$^-$ compared to that in wild-type cells, suggesting that the Sca1 complex controls RasC signaling in vegetatively growing amoebae as well as in the developed cells (Figure S3B), consistent with random motility defects in vegetative amoebae (Figure 2C).

To assess which Ras effector pathway contributes to the RasC-regulated PKB activity downstream from the Sca1 complex, we first tested the chemoattractant-induced activity of PI3K in live cells using a fluorescent PI(3,4,5)P_3 reporter consisting of the pleckstrin homology domain of the cytosolic regulator of adenylyl cyclase fused to GFP (PHcrac-GFP) (Dormann et al., 2002; Parent et al., 1998). As shown in Figures 3E and 3F, the production and accumulation of PI(3,4,5)P_3 in *scaA*$^-$ cells, at both the leading edge in chemotaxing cells and uniformly along the plasma membrane upon global chemoattractant stimulation, are similar to those in wild-type cells. In contrast, when evaluating the chemoattractant-induced activity of TORC2 by assessing the phosphorylation of PKB and PKBR1 at their hydrophobic motif (Kamimura et al., 2008), we found that TORC2 activity is decreased in *scaA*$^-$ compared to that in wild-type cells (Figure 3G). These findings suggest that the Sca1 complex-regulated RasC activation modulates the activity of TORC2 and not PI3K.

Using a fluorescent reporter for Ras activity [Ras binding domain (RBD) of human Raf1 fused to GFP], which binds active RasG but not RasC, we showed previously that active RasG (RasG-GTP) is enriched at the leading edge of migrating cells (Kae et al., 2004; Sasaki et al., 2004; Zhang et al., 2008). However, the localization of active RasC remains unknown. Therefore, to better understand the regulation of RasC's function by the Sca1 complex, we studied the localization of a GFP-Sca1 fusion protein, which complements the *scaA*$^-$ phenotypes (data not shown). As illustrated in Figure 4A, GFP-Sca1 is mostly found in the cytosol of resting cells but a fraction is recruited to the plasma membrane upon uniform chemoattractant stimulation, peaking ~6 s after stimulation. Interestingly, GFP-Sca1 does not undergo chemoattractant-induced membrane translocation in cells that lack Aimless and RasGEFH, which suggests that the RasGEFs and/or PHR are required for the recruitment of the complex to the plasma membrane. To investigate the mechanisms regulating the localization of the Sca1 complex, we assessed the effect of inhibiting F-actin polymerization and PI3K on the membrane translocation of GFP-Sca1 using Latrunculin B (LatB) and LY294002, respectively. Whereas cells treated with LY294002 actually displayed increased and prolonged GFP-Sca1 translocation, LatB treatment inhibited the membrane translocation of GFP-Sca1 (Figure 4B). Consistent with these

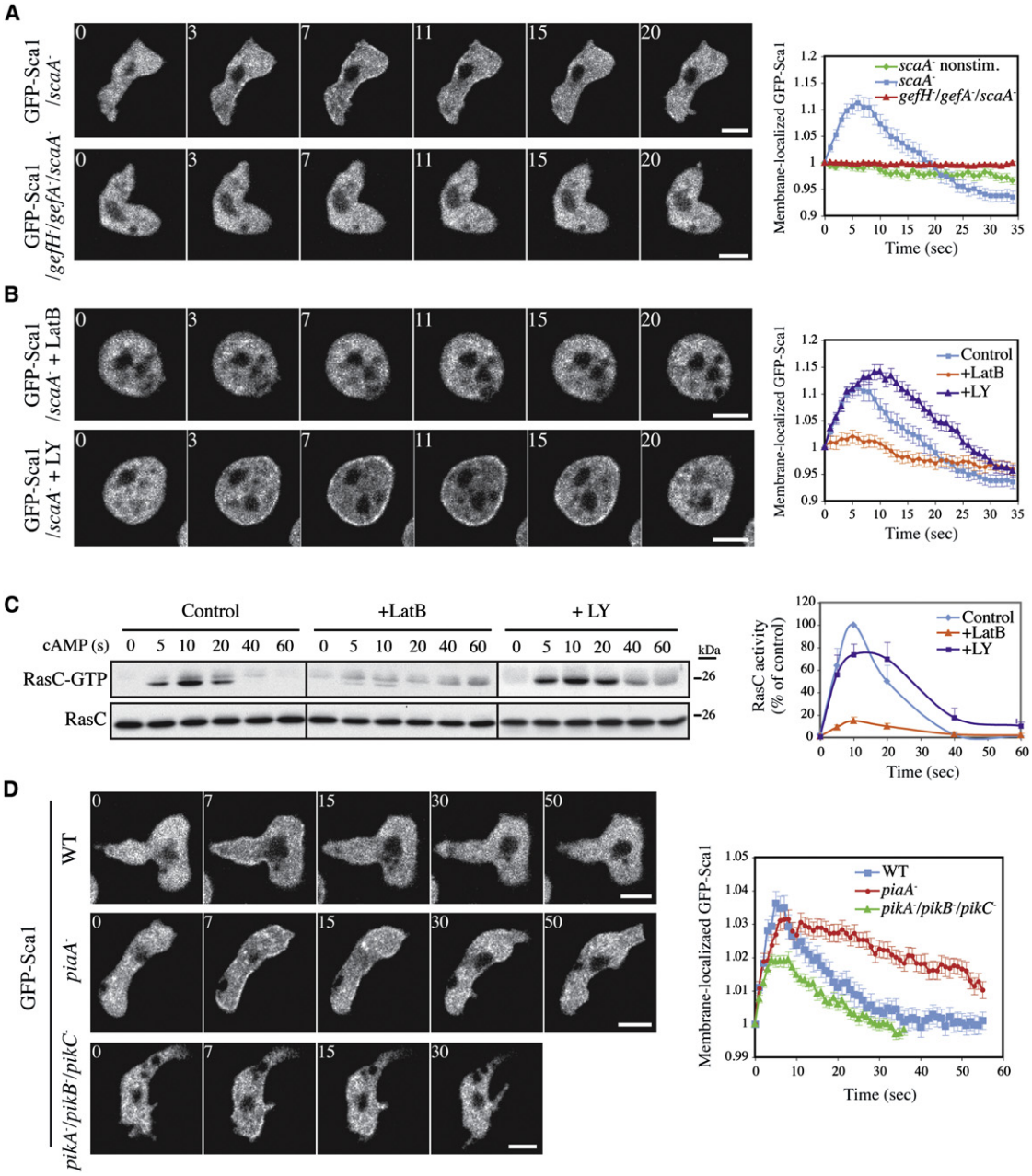

Figure 4. Sca1 Transiently Localizes to the Plasma Membrane in a Chemoattractant- and Actin-Dependent Manner and Is Negatively Regulated by TORC2

(A) Live imaging of GFP-Sca1, expressed in either *scaA*$^-$ or *gefH*$^-$/*gefA*$^-$/*scaA*$^-$, upon uniform cAMP stimulation. Numbers represent time after stimulation in seconds. The relative membrane fluorescence intensity of GFP-Sca1 is shown on the right.

(B) Cells were treated with 15 μM LatB or 60 μM LY294002 for 30 min prior cAMP stimulation.

(C) cAMP-induced RasC activity was assessed as described in Figure 3A, following LatB and LY294002 treatments. Quantification of data, expressed as a percentage of the 10 s time point (max) for the control, is shown on the right. Data represent mean ± SD of two independent experiments.

(D) Live imaging of GFP-Sca1 expressed in wild-type (WT), *piaA*$^-$, or *pikA*$^-$/*pikB*$^-$/*pikC*$^-$ cells. All imaging data represent mean ± SEM of ≥25 measurements performed on ≥20 cells from three independent experiments, and scale bars represent 5 μm. See also Figure S4.

observations, we found that LatB inhibits and LY294002 slightly prolongs chemoattractant-mediated RasC activation (Figure 4C). LY294002 was previously suggested to inhibit TORC2 in addition to PI3K and we observed that the inhibitor did inhibit ~30% of TORC2 activity under the conditions used for the GFP-Sca1 translocation assay (Figure S4) (Brunn et al., 1996; Kamimura et al., 2008). Therefore, to directly address the role of PI3K and TORC2 in the regulation of GFP-Sca1's localization, we assessed the membrane translocation of GFP-Sca1 in cells lacking either Pianissimo (TORC2 component and ortholog

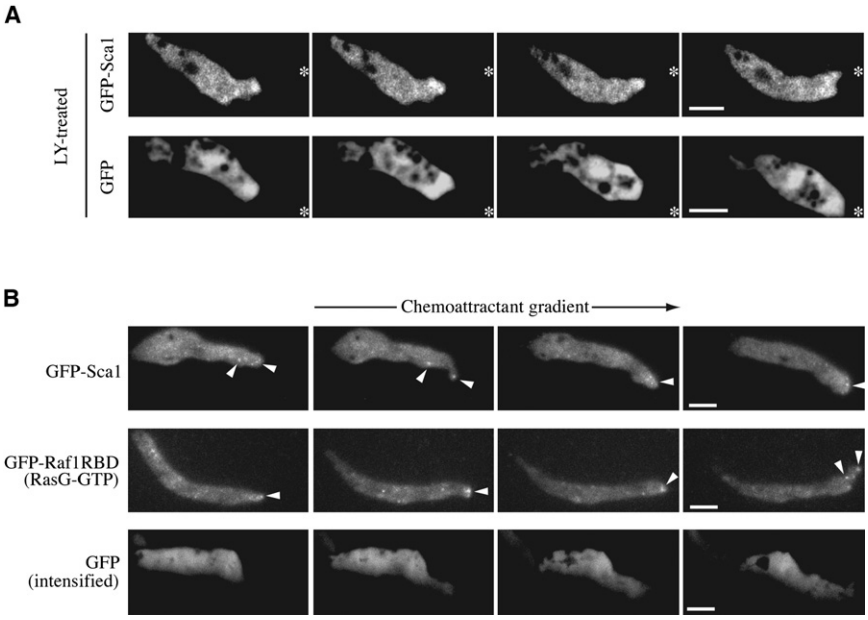

Figure 5. Sca1 Is Enriched at the Leading Edge of Chemotaxing Cells

(A) Live imaging of LY294002-treated *scaA*$^-$ cells expressing GFP-Sca1 or wild-type cells expressing soluble GFP and migrating in an exponential gradient of cAMP delivered by a micropipette. Asterisk shows position of the micropipette.

(B) *scaA*$^-$ cells expressing GFP-Sca1 or wild-type cells expressing either the RasG-GTP reporter (GFP-Raf1RBD) or soluble GFP and migrating under agar in a cAMP gradient were imaged by TIRFM. Signal from the soluble GFP had to be intensified in order to be visualized. Arrows mark regions of enriched fluorescence. Scale bars represent 5 μm.

of mammalian Rictor) or PI3K1, 2, and 3. With the presence of endogenous Sca1 in these strains and wild-type cells, the level of GFP-Sca1 translocation is smaller than that in *scaA*$^-$; however, we clearly observed that the membrane translocation of GFP-Sca1 in *piaA*$^-$ was considerably prolonged, whereas it was slightly reduced in *pikA*$^-$/*pikB*$^-$/*pikC*$^-$ compared to that in wild-type cells (Figure 4D). These findings suggest that while an intact actin cytoskeleton is required for the transient chemoattractant-dependent localization of the Sca1 complex at the plasma membrane, and therefore RasC activation, TORC2 signaling plays a negative regulatory role.

Attempts to determine the localization of GFP-Sca1 in chemotaxing cells using conventional confocal microscopy have been unsuccessful, possibly because the amount of GFP-Sca1 localized at the membrane compared to the cytosol at any given time is too low to be clearly visualized. However, cells pretreated with LY294002, which increases the cAMP-induced GFP-Sca1 membrane translocation (Figure 4A), exhibit an enrichment of GFP-Sca1 at the leading edge in contrast to LY294002-treated cells expressing only GFP (Figure 5A). To assess the localization of GFP-Sca1 during chemotaxis under normal conditions, we turned to total internal reflection fluorescence microscopy (TIRFM), which provides a higher signal-to-noise ratio and allows visualization of proteins at or near the plasma membrane only (Axelrod, 2001). Using TIRFM imaging and cells chemotaxing under agar to insure uniformly flat cells, we confirmed that GFP-Sca1 is periodically enriched at the plasma membrane of extending pseudopodia and at the leading edge of chemotaxing cells (Figure 5B). Moreover, we observed that GFP-Sca1 displays two different patterns of membrane localization within the protrusion: it is found either uniformly distributed or transiently enriched in discrete regions appearing as dots that persist for no more than 4 s at a time. In contrast, cells expressing soluble GFP display a smooth and uniform signal that could only be detected with longer exposures. Interestingly, when assessed in TIRFM, the RasG activity reporter GFP-Raf1RBD revealed membrane localization patterns similar to those of GFP-Sca1 (Figure 5B). These findings suggest that the Sca1 complex promotes RasC activation at the leading edge of chemotaxing cells in regions similar to those of enriched RasG-GTP.

TORC2 and PKB/PKBR1 Regulate RasC Activity Via Negative Feedback

The presence of PP2A in the Sca1 complex suggests that the complex's function is tightly regulated by phosphorylation. We performed phosphoproteomic studies on samples from unstimulated cells and cells stimulated with chemoattractant for either 10 or 60 s and found that Sca1 undergoes dynamic phosphorylation. One phosphorylation site in particular (S359), detected only at 10 s after stimulation, is within a PKB phosphorylation consensus motif (RXRXXS/T; Alessi et al., 1996) (Figure 6A). We then analyzed the PKB phosphorylation of immunopurified Sca1 by western blot, using an anti-phospho-PKB substrate antibody (αP-PKBS). As shown in Figure 6B, the PKBS antibody allows detection of transient chemoattractant-induced phosphorylation of Sca1, with a peak at ~5–10 s after stimulation, which correlates with the phosphoproteomics data. Furthermore, we found that this Sca1 phosphorylation is reduced in cells lacking PKB (*pkbA*$^-$), reduced to a greater extent in *pkbr1*$^-$ cells, and abolished in cells lacking both kinases (Figure 6C). Our findings suggest that Sca1 undergoes chemoattractant-regulated PKB/PKBR1-mediated phosphorylation. We further found that Sca1 is not phosphorylated in *piaA*$^-$ cells, suggesting TORC2 is required for this response (data not shown). Given that PKB/PKBR1 mediates cAMP production, and consequently lies upstream from PKA, we assessed whether part of the phosphorylation signal is PKA dependent. Unexpectedly, we found that both the basal and chemoattractant-induced phosphorylation of Sca1 are increased in PKA catalytic null cells (*pkaC*$^-$) compared to that in wild-type cells (Figure 6C). Therefore, these observations suggest that whereas the PKB/PKBR1-dependent phosphorylation of Sca1 occurs

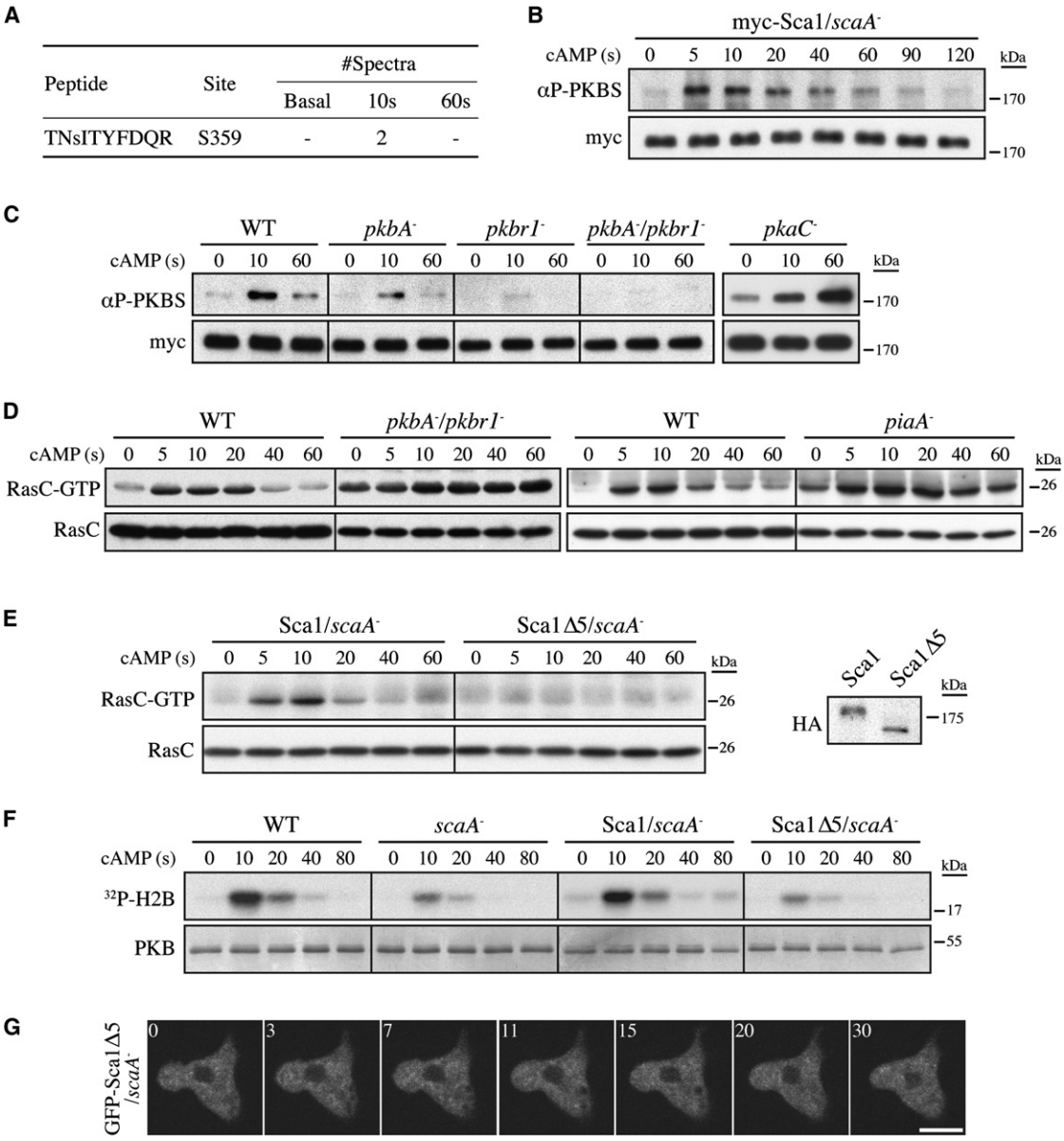

Figure 6. The Function of the Sca1 Complex Is Regulated by TORC2 and PKB/PKBR1 in a Negative Feedback Fashion and by PP2A

(A) Phosphoproteomics analysis allowed identification of Sca1 phosphorylation at serine 359 (S359). Two spectra corresponding to the indicated phosphopeptide were obtained from a sample stimulated for 10 s with cAMP.

(B and C) cAMP-induced phosphorylation of immunoprecipitated myc-tagged Sca1 expressed in the indicated strains was assessed by immunoblotting with an anti-phospho-Akt/PKB substrate antibody (αP-PKBS).

(D and E) cAMP-induced RasC activity in the indicated strains was assessed as described in Figure 3A. Expression of HHF-Sca1 and -Sca1Δ5 was controlled by HA immunoblotting.

(F) cAMP-induced PKB kinase activity was assessed as described in Figure 3B.

(G) Live imaging of GFP-Sca1Δ5 upon uniform cAMP stimulation. Numbers represent time after stimulation in seconds. Scale bar represents 5 μm. Data are representative of at least two independent experiments.

independently of PKA, PKA is involved in the regulation of this pathway.

Since the Sca1-controlled RasC activity promotes the activation of PKB/PKBR1 through regulation of TORC2, PKB/PKBR1-mediated phosphorylation of Sca1 suggests the presence of a regulatory feedback mechanism. To investigate this possible feedback loop, we assessed the activation of RasC in *pkbA*$^{-}$/*pkbr1*$^{-}$ and *piaA*$^{-}$ cells. Surprisingly, we found that not only is the basal level of RasC activity elevated in both *pkbA*$^{-}$/*pkbr1*$^{-}$ and *piaA*$^{-}$ compared to that in wild-type cells but also that chemoattractant-induced RasC activation is considerably increased and fails to rapidly adapt as it normally does by 40 s after stimulation (Figure 6D). Consequently, these findings suggest that TORC2 and PKB/PKBR1 regulate RasC

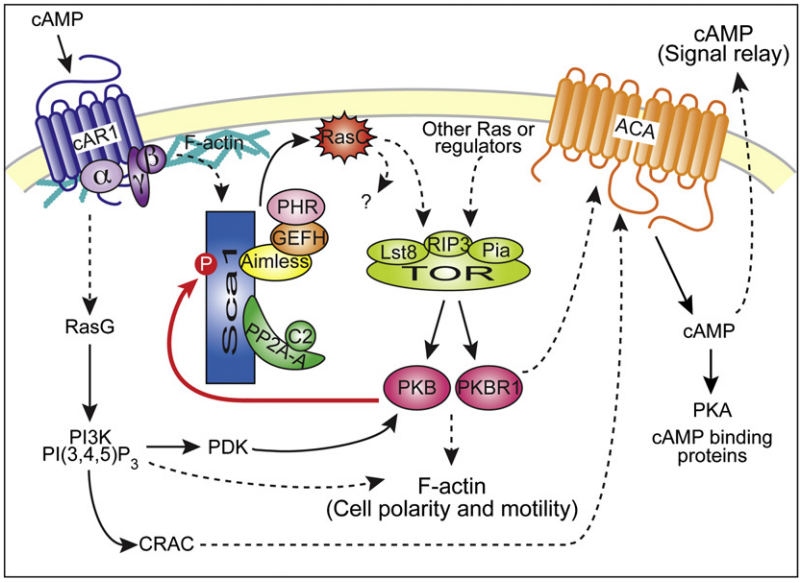

Figure 7. Regulation of RasC Signaling during Chemotaxis

Chemoattractant stimulation promotes the F-actin-dependent recruitment of the Sca1 complex to the plasma membrane and the subsequent activation of the RasC-TORC2-PKB/PKBR1 pathway at the leading edge of chemotaxing cells. This signaling pathway controls cAMP production and leads to modulation of the F-actin cytoskeleton, thereby regulating signal relay and cell motility, respectively. The RasG-PI3K pathway appears to regulate F-actin, ACA (via CRAC), and PKB independently of the RasC-TORC2 pathway, and other regulators and/or Ras proteins control TORC2 activity in addition to RasC. It is also possible that RasC has other effectors. TORC2 and PKB/PKBR1 regulate RasC activity in a negative feedback fashion that involves regulation of the Sca1 complex's localization through phosphorylation of Sca1. PP2A seems to be necessary for the function of the Sca1 complex, possibly for the dynamic regulation of the complex by phosphorylation.

activation in a negative feedback fashion, which might involve direct regulation of the Sca1 complex by PKB/PKBR1.

To obtain insight into the role of PP2A in the Sca1 complex, we used the Sca1 deletion mutant Sca1Δ5 that disrupts the interaction of the scaffold with PP2A but still associates with the RasGEFs and PHR (Figures 1I and 1J and Figure S1B). Sca1Δ5 fails to rescue the chemoattractant-induced activation of RasC and PKB in *scaA*$^-$ and does not translocate to the plasma membrane upon uniform chemoattractant stimulation (Figures 6E–6G). These observations suggest that PP2A is essential for the function of the Sca1 complex, possibly by controlling its translocation to the cortex.

DISCUSSION

Significant progress has been made toward identifying genes implicated in chemotaxis, but little is known about the molecular mechanisms that spatiotemporally control chemotactic signaling. Our study sheds light on one of these mechanisms that involves the identified Sca1/RasGEF/PP2A signaling complex, which controls the RasC-TORC2-PKB/PKBR1 pathway at the leading edge of chemotaxing cells, and reveals that RasC signaling is tightly controlled through TORC2- and PKB/PKBR1-mediated negative feedback regulation (Figure 7).

Our pull-down and coimmunoprecipitation experiments suggest that Aimless, RasGEFH, and Sca1 form a single, stable complex that also includes PHR and the PP2A core enzyme PP2A-A/C2. These experiments, together with Sca1's lack of a known enzymatic domain, strongly suggest that Sca1 is a scaffolding protein. Although Sca1 does not appear to be evolutionarily conserved, we found that the *Dictyostelium* genome encodes a Sca1-related protein, designated Sca2 (DDB_G0267776). Interestingly, we have preliminary data suggesting that Sca2 also associates with two LisH domain-containing RasGEFs, RasGEF-F and RasGEFI (Wilkins et al., 2005), as well as the PP2A-A/C2 core enzyme (S. Lee, P.G.C., and R.A.F., unpublished data). We do not yet know which Ras proteins are regulated by RasGEF-F and RasGEFI, but it appears that the Sca2 complex regulates different cellular functions than those controlled by the Sca1 complex. Thus, the existence of RasGEF-containing complexes extends beyond the Sca1 complex described here, although its presence in other organisms is unknown. It is possible that, even if Sca1 and Sca2 are not conserved outside of *Dictyostelium*, their functions are. It is interesting that no PP2A regulatory B subunits were found associated with the Sca1 complex under either unstimulated or stimulated conditions (data not shown). It is possible that the interaction of the regulatory B subunit with the core PP2A dimer in the Sca1 complex is too weak and/or transient to allow its detection in our pull-down experiments.

The developmental, chemotaxis, and random cell motility phenotypes of *gefA*$^-$, *gefH*$^-$/*gefA*$^-$, and *scaA*$^-$ are extremely similar to those of *rasC*$^-$, which is consistent with the primary role of the Sca1 complex in promoting RasC activation (Lim et al., 2001, 2005). In addition, our data indicate that most of the Sca1 complex's GEF activity toward RasC is provided by Aimless, but RasGEFH also plays a role. Indeed, we repeatedly observed that chemoattractant-induced RasC activation is reduced in *gefH*$^-$, and we sometimes observed residual RasC activation in *gefA*$^-$, which is then lost in *gefH*$^-$/*gefA*$^-$. These observations suggest that RasGEFH is essential for full activation of RasC by Aimless and may have some GEF activity toward RasC. Whether RasGEFH interacts with another LisH domain-containing RasGEF, or complex, in the absence of Aimless is unknown. It is also unclear whether RasGEFH and PHR always interact and what role PHR plays in the complex. However, the fact that the phenotypes of *phr*$^-$ cells differ from those of *gefH*$^-$, while PHR associates with the Sca1 complex by interacting with RasGEFH, suggests that PHR might have a separate function in addition to that linked to the Sca1 complex. Alternatively, PHR might play an intricate regulatory role in the Sca1 complex's function, which does not require direct interaction with the complex. We are currently investigating these possibilities.

As was previously suggested for Aimless (Insall et al., 1996), we found that the Sca1 complex controls both F-actin polymerization and cAMP production (signal relay), which explains the cell motility and aggregation defects of the Sca1 complex null mutants. However, whereas cAMP accumulation correlates with the level of RasC activity in Sca1 complex null cells, considerable levels of TORC2 and PKB activity remain in cells lacking *gefA* or *scaA*, which suggest that the Sca1 complex-regulated RasC activity only controls part of the chemoattractant-induced TORC2 and PKB activation. Interestingly, we found that PKB/PKBR1 is essential for the chemoattractant-induced accumulation of cAMP and that the Sca1 complex-regulated RasC activity controls PKB, and most likely also PKBR1, by regulating TORC2 and not PI3K. Whereas data suggest that PKBR1 is regulated solely by TORC2 and not PI(3,4,5)P_3 signaling, PKB is regulated by both (Kamimura et al., 2008; Lee et al., 2005; Meili et al., 1999, 2000). Thus, PKB activity seems to be controlled by at least two parallel Ras pathways: a RasG-PI3K and a RasC-TORC2 pathway (Figure 7). Given our previous finding that the homolog of the human TORC2 component Sin1, RIP3, interacts with RasG in vitro, perhaps RasG, in addition to controlling PI3K, also controls TORC2 activity in vivo (Lee et al., 1999). We previously suggested that RIP3 did not bind to RasC in yeast two-hybrid assays; however, more recent studies suggest that this may have been due to a very poor expression of RasC in this yeast two-hybrid system (data not shown). Because some TORC2 activity was reported to remain in *rasC*$^-$/*rasG*$^-$ cells, TORC2 also appears to have other, yet unknown, upstream regulators (Kamimura et al., 2008). Altogether, these observations indicate that TORC2 and PKB/PKBR1 are important signal integrators, coordinating cell motility and chemotaxis with signal relay during aggregation. The Sca1 complex-mediated RasC activation thus provides a common link between these chemoattractant responses that must be coordinated for efficient aggregation.

The absence of chemoattractant-induced RasC activity in *scaA*$^-$ cells suggests that the integrity of the Sca1 complex is crucial and controls the function of the associated RasGEFs. Intriguingly, whereas chemoattractant-induced RasC activity is absent in both *gefH*$^-$/*gefA*$^-$ and *scaA*$^-$, we consistently observed that PKB's activity is lower in *scaA*$^-$ than that in *gefH*$^-$/*gefA*$^-$. Although this discrepancy could simply be due to a difference in sensitivity between the assays, it is also possible that Sca1 interacts with other RasGEFs in the absence of Aimless, leading to some Sca1-dependent regulation of PKB activity through activation of a Ras protein other than RasC, in *gefA*$^-$ and *gefH*$^-$/*gefA*$^-$, which is then lost upon disruption of *scaA*. In support of this hypothesis, we found that some RasGEF-F copurifies with Sca1 when Sca1 is expressed in *gefH*$^-$/*gefA*$^-$/*scaA*$^-$, although very little RasGEF-F is detected in this pull-down compared to the amount of Aimless and RasGEFH usually copurified with Sca1 (data not shown).

The relatively weak enrichment of Sca1 to the plasma membrane upon uniform chemoattractant stimulation and to the leading edge of migrating cells is consistent with Ras activation being very upstream in the chemoattractant signaling pathways, which is thought to occur immediately downstream from the receptors and heterotrimeric G proteins and prior to signal amplification. Using LY294002-treated cells as well as TIRFM imaging, we were able to see that Sca1 is enriched at the leading edge membrane of chemotaxing cells and to sites similar to those of a RasG-GTP reporter. Previously, with the lack of in vivo reporter for RasC activity, the general assumption was that RasC-GTP must localize at the back of migrating cells, where ACA is enriched (Kriebel et al., 2003, 2008). However, the findings that the Sca1 complex is enriched at the leading edge and that RasC regulates TORC2, whose activity was recently suggested to be restricted to the leading edge (Kamimura et al., 2008), strongly support that RasC-GTP also localizes to the front of chemotaxing cells. As we also found that PKB/PKBR1 is necessary for ACA activation, we suggest that a soluble PKB/PKBR1 substrate is implicated in linking the RasC-TORC2-PKB/PKBR1 pathway to the activation of ACA.

The mechanism by which the Sca1 complex is recruited to the plasma membrane upon chemoattractant stimulation remains to be determined; however, our findings suggest that translocation of the complex requires the RasGEFs and/or PHR, as well as an intact actin cytoskeleton, and is negatively regulated in a TORC2-PKB/PKBR1-dependent fashion, most likely implicating direct PKB/PKBR1 phosphorylation of Sca1. We are currently investigating potential PHR-, Aimless-, and RasGEFH-interacting proteins that might act in the recruitment of Sca1 to the plasma membrane and promote activation of the RasGEFs. One possibility is that the RasGEFs directly interact with the activated heterotrimeric G proteins. The role of the actin cytoskeleton in the membrane translocation of Sca1 is unknown, but, considering the fast kinetics of the recruitment, we suggest that the membrane recruitment of Sca1 requires an originally intact actin cortex rather than the chemoattractant-induced F-actin polymerization. In addition, our data suggest that TORC2 and PKB/PKBR1 regulate the activity of RasC in a negative feedback fashion by modulating the localization of the Sca1 complex. Most likely, this includes direct phosphorylation of Sca1 by PKB/PKBR1 and requires TORC2 function but appears to be independent of PI3K signaling. Since PI3K is upstream of PKB and not PKBR1 (Kamimura et al., 2008; Lee et al., 2005; Meili et al., 1999, 2000), these observations suggest that PKBR1 might have a prominent role in the feedback regulation of RasC activity, as well as the possibility of compartmentalization of the RasC-TORC2-PKB/PKBR1 pathway, consistent with the relative effect of PKB/PKBR1 knockouts on Sca1 phosphorylation.

We found that Sca1 is phosphorylated by PKB/PKBR1 at S359. However, site-directed mutagenesis studies suggest the presence of additional PKB phosphorylation sites in Sca1, which remain to be identified (data not shown). Hence, regulation of the Sca1 complex by PKB/PKBR1 may be considerably more intricate. Also, in addition to regulating the Sca1 complex, TORC2 and PKB/PKBR1 might act at multiple levels of the pathway upstream of RasC in order to efficiently attenuate RasC activity. Moreover, we found evidence that PKA negatively regulates the PKB/PKBR1-dependent phosphorylation of Sca1. We are currently investigating the mechanism underlying the regulation of Sca1 phosphorylation by PKA, but preliminary data suggest that it occurs independently of ACA, which is consistent with previously reported observations that ACA is not required to provide intracellular cAMP for PKA activation (Pitt et al., 1993; Kim et al., 1998).

Scaffold-mediated assembly of multiprotein complexes has been implicated in the control of mitogen-activated protein

(MAP) kinases as well as cAMP signaling pathways in mammalian cells (Brown and Sacks, 2009; Carnegie et al., 2009). Studies performed in different biological systems have shown that scaffolds exert substantial spatiotemporal control of MAP kinase signaling, thereby influencing the kinase selectivity toward substrates and determining the biological outcome (Casar et al., 2009; Claperon and Therrien, 2007). Whether the Sca1 complex provides specificity in addition to spatiotemporal control of RasC signaling remains to be determined. However, many aspects of the Sca1 complex are reminiscent of the well-described MAP kinase scaffold kinase suppressor of Ras 1 (KSR1). KSR1 associates with PP2A, which is necessary for the KSR1-mediated activation of the ERK1/2 pathway, and KSR1's membrane localization and function are regulated by ERK-mediated negative feedback phosphorylation (McKay et al., 2009; Ory et al., 2003). Our observations suggest that the presence of PP2A in the Sca1 complex is essential to the complex's function and might regulate the localization of the complex. Further investigation is needed to fully understand the role of the phosphatase in the Sca1 complex, but PP2A may have a role similar to that in the KSR1 complex, promoting its resensitization through dephosphorylation of the scaffold.

In conclusion, our study uncovered a mechanism by which RasC and TORC2 are activated downstream from the receptor and heterotrimeric G protein and spatiotemporally controlled during chemotaxis. Our findings reveal that TORC2 and PKB/PKBR1 are part of an important adaptation mechanism controlling RasC signaling and signal relay, which is likely to play a central role in the global adaptation of cells that is essential to maintain responsiveness to the chemoattractant. The Sca1 complex RasC-TORC2-PKB/PKBR1 pathway functions biologically to regulate cell motility, chemotaxis, and the relay of the cAMP chemoattractant signal in *Dictyostelium* cells. The role and regulation of TORC2 is not yet understood in any system and, although aspects of this pathway may be unique to *Dictyostelium*, we suggest that our results may also provide general insights into how Ras and TORC2 pathways are spatially and temporally controlled downstream from G protein-coupled receptors in other systems.

EXPERIMENTAL PROCEDURES

Affinity Purification

For pull-down and coimmunoprecipitation assays, 10^8 cells were lysed in 1 ml HEPES-DSP lysis buffer [50 mM HEPES (pH 7.2), 0.5% NP-40, 150 mM NaCl, 10% glycerol, and 2 mM DSP, with phosphatase and protease inhibitors (10 mM NaF, 1 mM sodium-orthovanadate, 25 mM β-glycerophosphate, 3 mM sodium-pyrophosphate, 1 mM PMSF, 5 μg/ml leupeptin, and 5 μg/ml aprotinin)], followed by quenching of the crosslinker with 150 mM Tris (pH 7.4). For simple immunoprecipitation, cells were lysed in Tris lysis buffer [50 mM Tris (pH 7.6), 1% NP-40, 100 mM NaCl, 1 mM EDTA, 10% glycerol, and 1 mM DTT, with phosphatase and protease inhibitors]. For cAMP-stimulated samples, cells were lysed with 2× lysis buffer at the indicated time after stimulation with 1 μM cAMP and cleared by centrifugation. Samples were then subjected to sequential FLAG-His purification (pull-downs) and analyzed by mass spectrometry or immunopurified with the indicated agarose-coupled antibodies, resolved on SDS-PAGE, and analyzed by western blot.

Mass Spectrometry and Phosphopeptide Analysis

Analysis of the protein samples by mass spectrometry was performed as described previously (Para et al., 2009). For the phosphoproteomics assay, 4×10^8 developed cells were washed, resuspended in 20 mM MES (pH 6.8), and then stimulated for either 10 or 60 s with 10 μM cAMP, and the stimulations were stopped by adding an equal volume of cold 2× HBS buffer [20 mM HEPES (pH 7.4), 300 mM NaCl, 4% *Rapi*Gest (Waters), 0.4 mM sodium-orthovanadate, 10 mM β-glycerophosphate, 4 mM NaF, and 1.2 mM sodium-pyrophosphate] and plunging the samples in lN_2. The samples were then thawed on ice and solubilized by sonication. Protein samples were diluted four times with 25 mM HEPES buffer (pH 7.2) and 10 mg of protein/sample was reduced, alkylated, and digested with trypsin. The samples were incubated with 1% TFA (pH 1.4) for 16 hr at 4°C to precipitate *Rapi*Gest and cleared by filtration. Phosphopeptides were enriched using homemade TiO_2 columns and acidified prior to LC-MS/MS analysis.

Biochemical Assays

Chemoattractant-induced production of cAMP, Ras activity, PKB kinase activity, and F-actin measurements were performed as described previously (Insall et al., 1996; Meili et al., 1999; Sasaki et al., 2004, 2007; Van Haastert, 2006; Zhang et al., 2008). We assessed TORC2 activity by evaluating the TORC2-mediated phosphorylation of PKB and PKBR1. Briefly, 10^8 aggregation-competent cells were washed and desensitized for 20 min in 12 mM sodium/potassium phosphate buffer before cAMP stimulation. We immunoprecipitated PKB while using total cell lysates to assess PKBR1 phosphorylation. The samples were resolved on SDS-PAGE and phosphorylation of the kinases' hydrophobic motif was detected using anti-phospho-(Ser/Thr) PDK1 docking motif (18A2) as described previously (Kamimura et al., 2008). cAMP and folate were both used at 1 μM final concentration.

Chemotaxis, Global Responses, and Cell Motility Assays

Assessment of chemotaxis, global responses to cAMP, and vegetative cell motility, as well as analysis using the DIAS software, have been described elsewhere (Chung and Firtel, 1999; Sasaki et al., 2007; Wessels and Soll, 1998). We performed chemotaxis under agar as previously described (Andrew and Insall, 2007). Image acquisition and analysis were performed as described previously (Zhang et al., 2008).

Additional procedures, including the cell culture and molecular biology methods, as well as a list of reagents, can be found in the Supplemental Experimental Procedures.

SUPPLEMENTAL INFORMATION

Supplemental information includes four figures, one table, one movie, Supplemental Experimental Procedures, and Supplemental References and can be found with this article online at doi:10.1016/j.devcel.2010.03.017.

ACKNOWLEDGMENTS

We thank the Firtel laboratory members for their technical support, constructive discussions, and critical reading of the manuscript; C. Janetopoulos for sharing his protocol on preparation and folate stimulation of vegetative cells; and H. Hakozaki and O. Kwon for assistance with TIRF imaging, which was conducted at the National Center for Microscopy and Imaging Research at the University of California, San Diego, supported by National Institutes of Health Research Resource Grant P41 RR04050 to M. Ellisman. P.G.C. was supported, in part, by a fellowship from the Fonds de la Recherche en Santé du Québec. This work was supported by USPS grant R01 GM037830 to R.A.F. and P01 GM078586.

Received: September 11, 2009
Revised: January 25, 2010
Accepted: March 3, 2010
Published: May 17, 2010

REFERENCES

Affolter, M., and Weijer, C.J. (2005). Signaling to cytoskeletal dynamics during chemotaxis. Dev. Cell *9*, 19–34.

Alessi, D.R., Caudwell, F.B., Andjelkovic, M., Hemmings, B.A., and Cohen, P. (1996). Molecular basis for the substrate specificity of protein kinase B; comparison with MAPKAP kinase-1 and p70 S6 kinase. FEBS Lett. *399*, 333–338.

Andrew, N., and Insall, R.H. (2007). Chemotaxis in shallow gradients is mediated independently of PtdIns 3-kinase by biased choices between random protrusions. Nat. Cell Biol. *9*, 193–200.

Annesley, S.J., and Fisher, P.R. (2009). *Dictyostelium discoideum*—a model for many reasons. Mol. Cell. Biochem. *329*, 73–91.

Axelrod, D. (2001). Total internal reflection fluorescence microscopy in cell biology. Traffic *2*, 764–774.

Bolourani, P., Spiegelman, G.B., and Weeks, G. (2006). Delineation of the roles played by RasG and RasC in cAMP-dependent signal transduction during the early development of *Dictyostelium discoideum*. Mol. Biol. Cell *17*, 4543–4550.

Brown, M.D., and Sacks, D.B. (2009). Protein scaffolds in MAP kinase signalling. Cell. Signal. *21*, 462–469.

Brunn, G.J., Williams, J., Sabers, C., Wiederrecht, G., Lawrence, J.C., and Abraham, R.T. (1996). Direct inhibition of the signaling functions of the mammalian target of rapamycin by the phosphoinositide 3-kinase inhibitors, wortmannin and LY294002. EMBO J. *15*, 5256–5267.

Carnegie, G.K., Means, C.K., and Scott, J.D. (2009). A-kinase anchoring proteins: from protein complexes to physiology and disease. IUBMB Life *61*, 394–406.

Casar, B., Arozarena, I., Sanz-Moreno, V., Pinto, A., Agudo-Ibanez, L., Marais, R., Lewis, R.E., Berciano, M.T., and Crespo, P. (2009). Ras subcellular localization defines extracellular signal-regulated kinase 1 and 2 substrate specificity through distinct utilization of scaffold proteins. Mol. Cell. Biol. *29*, 1338–1353.

Chung, C.Y., and Firtel, R.A. (1999). PAKa, a putative PAK family member, is required for cytokinesis and the regulation of the cytoskeleton in *Dictyostelium discoideum* cells during chemotaxis. J. Cell Biol. *147*, 559–576.

Claperon, A., and Therrien, M. (2007). KSR and CNK: two scaffolds regulating RAS-mediated RAF activation. Oncogene *26*, 3143–3158.

Dormann, D., Weijer, G., Parent, C.A., Devreotes, P.N., and Weijer, C.J. (2002). Visualizing PI3 kinase-mediated cell-cell signaling during *Dictyostelium* development. Curr. Biol. *12*, 1178–1188.

Funamoto, S., Meili, R., Lee, S., Parry, L., and Firtel, R.A. (2002). Spatial and temporal regulation of 3-phosphoinositides by PI 3-kinase and PTEN mediates chemotaxis. Cell *109*, 611–623.

Gerlitz, G., Darhin, E., Giorgio, G., Franco, B., and Reiner, O. (2005). Novel functional features of the Lis-H domain: role in protein dimerization, half-life and cellular localization. Cell Cycle *4*, 1632–1640.

Huang, Y.E., Iijima, M., Parent, C.A., Funamoto, S., Firtel, R.A., and Devreotes, P. (2003). Receptor-mediated regulation of PI3Ks confines PI(3,4,5)P3 to the leading edge of chemotaxing cells. Mol. Biol. Cell *14*, 1913–1922.

Insall, R.H., Borleis, J., and Devreotes, P.N. (1996). The aimless RasGEF is required for processing of chemotactic signals through G-protein-coupled receptors in *Dictyostelium*. Curr. Biol. *6*, 719–729.

Janssens, V., Longin, S., and Goris, J. (2008). PP2A holoenzyme assembly: *in cauda venenum* (the sting is in the tail). Trends Biochem. Sci. *33*, 113–121.

Kae, H., Lim, C.J., Spiegelman, G.B., and Weeks, G. (2004). Chemoattractant-induced Ras activation during *Dictyostelium* aggregation. EMBO Rep. *5*, 602–606.

Kae, H., Kortholt, A., Rehmann, H., Insall, R.H., Van Haastert, P.J., Spiegelman, G.B., and Weeks, G. (2007). Cyclic AMP signalling in *Dictyostelium*: G-proteins activate separate Ras pathways using specific RasGEFs. EMBO Rep. *8*, 477–482.

Kamimura, Y., Xiong, Y., Iglesias, P.A., Hoeller, O., Bolourani, P., and Devreotes, P.N. (2008). PIP3-independent activation of TorC2 and PKB at the cell's leading edge mediates chemotaxis. Curr. Biol. *18*, 1034–1043.

Kim, H.J., Chang, W.T., Meima, M., Gross, J.D., and Schaap, P. (1998). A novel adenylyl cyclase detected in rapidly developing mutants of *Dictyostelium*. J. Biol. Chem. *273*, 30859–30862.

Kriebel, P.W., Barr, V.A., and Parent, C.A. (2003). Adenylyl cyclase localization regulates streaming during chemotaxis. Cell *112*, 549–560.

Kriebel, P.W., Barr, V.A., Rericha, E.C., Zhang, G., and Parent, C.A. (2008). Collective cell migration requires vesicular trafficking for chemoattractant delivery at the trailing edge. J. Cell Biol. *183*, 949–961.

Lee, S., Parent, C.A., Insall, R., and Firtel, R.A. (1999). A novel Ras-interacting protein required for chemotaxis and cyclic adenosine monophosphate signal relay in *Dictyostelium*. Mol. Biol. Cell *10*, 2829–2845.

Lee, S., Comer, F.I., Sasaki, A., McLeod, I.X., Duong, Y., Okumura, K., Yates, J.R., 3rd, Parent, C.A., and Firtel, R.A. (2005). TOR complex 2 integrates cell movement during chemotaxis and signal relay in *Dictyostelium*. Mol. Biol. Cell *16*, 4572–4583.

Lim, C.J., Spiegelman, G.B., and Weeks, G. (2001). RasC is required for optimal activation of adenylyl cyclase and Akt/PKB during aggregation. EMBO J. *20*, 4490–4499.

Lim, C.J., Zawadzki, K.A., Khosla, M., Secko, D.M., Spiegelman, G.B., and Weeks, G. (2005). Loss of the *Dictyostelium* RasC protein alters vegetative cell size, motility and endocytosis. Exp. Cell Res. *306*, 47–55.

Mateja, A., Cierpicki, T., Paduch, M., Derewenda, Z.S., and Otlewski, J. (2006). The dimerization mechanism of LIS1 and its implication for proteins containing the LisH motif. J. Mol. Biol. *357*, 621–631.

McKay, M.M., Ritt, D.A., and Morrison, D.K. (2009). Signaling dynamics of the KSR1 scaffold complex. Proc. Natl. Acad. Sci. USA *106*, 11022–11027.

Meili, R., Ellsworth, C., Lee, S., Reddy, T.B., Ma, H., and Firtel, R.A. (1999). Chemoattractant-mediated transient activation and membrane localization of Akt/PKB is required for efficient chemotaxis to cAMP in *Dictyostelium*. EMBO J. *18*, 2092–2105.

Meili, R., Ellsworth, C., and Firtel, R.A. (2000). A novel Akt/PKB-related kinase is essential for morphogenesis in *Dictyostelium*. Curr. Biol. *10*, 708–717.

Murphy, M.B., Levi, S.K., and Egelhoff, T.T. (1999). Molecular characterization and immunolocalization of *Dictyostelium discoideum* protein phosphatase 2A. FEBS Lett. *456*, 7–12.

Ory, S., Zhou, M., Conrads, T.P., Veenstra, T.D., and Morrison, D.K. (2003). Protein phosphatase 2A positively regulates Ras signaling by dephosphorylating KSR1 and Raf-1 on critical 14-3-3 binding sites. Curr. Biol. *13*, 1356–1364.

Para, A., Krischke, M., Merlot, S., Shen, Z., Oberholzer, M., Lee, S., Briggs, S., and Firtel, R.A. (2009). *Dictyostelium* Dock180-related RacGEFs regulate the actin cytoskeleton during cell motility. Mol. Biol. Cell *20*, 699–707.

Parent, C.A., Blacklock, B.J., Froehlich, W.M., Murphy, D.B., and Devreotes, P.N. (1998). G protein signaling events are activated at the leading edge of chemotactic cells. Cell *95*, 81–91.

Pitt, G.S., Brandt, R., Lin, K.C., Devreotes, P.N., and Schaap, P. (1993). Extracellular cAMP is sufficient to restore developmental gene expression and morphogenesis in *Dictyostelium* cells lacking the aggregation adenylyl cyclase (ACA). Genes Dev. *7*, 2172–2180.

Sasaki, A.T., and Firtel, R.A. (2006). Regulation of chemotaxis by the orchestrated activation of Ras, PI3K, and TOR. Eur. J. Cell Biol. *85*, 873–895.

Sasaki, A.T., Chun, C., Takeda, K., and Firtel, R.A. (2004). Localized Ras signaling at the leading edge regulates PI3K, cell polarity, and directional cell movement. J. Cell Biol. *167*, 505–518.

Sasaki, A.T., Janetopoulos, C., Lee, S., Charest, P.G., Takeda, K., Sundheimer, L.W., Meili, R., Devreotes, P.N., and Firtel, R.A. (2007). G protein-independent Ras/PI3K/F-actin circuit regulates basic cell motility. J. Cell Biol. *178*, 185–191.

Schroder, W.A., Buck, M., Cloonan, N., Hancock, J.F., Suhrbier, A., Sculley, T., and Bushell, G. (2007). Human Sin1 contains Ras-binding and pleckstrin homology domains and suppresses Ras signalling. Cell. Signal. *19*, 1279–1289.

Suire, S., Condliffe, A.M., Ferguson, G.J., Ellson, C.D., Guillou, H., Davidson, K., Welch, H., Coadwell, J., Turner, M., Chilvers, E.R., et al. (2006). Gbetagammas and the Ras binding domain of p110gamma are both important regulators of PI(3)Kgamma signalling in neutrophils. Nat. Cell Biol. *8*, 1303–1309.

Van Haastert, P.J. (2006). Analysis of signal transduction: formation of cAMP, cGMP, and Ins(1,4,5)P3 *in vivo* and *in vitro*. Methods Mol. Biol. *346*, 369–392.

Wessels, D., and Soll, D.R. (1998). Computer assisted analysis of cytoskeletal mutants of *Dictyostelium discoideum*. In Motion Analysis of Living Cells, D.R. Soll and D. Wessels, eds. (New York: John Wiley & Sons), pp. 101–140.

Wilkins, A., Szafranski, K., Fraser, D.J., Bakthavatsalam, D., Muller, R., Fisher, P.R., Glockner, G., Eichinger, L., Noegel, A.A., and Insall, R.H. (2005). The *Dictyostelium* genome encodes numerous RasGEFs with multiple biological roles. Genome Biol. *6*, R68.

Zhang, S., Charest, P.G., and Firtel, R.A. (2008). Spatiotemporal regulation of Ras activity provides directional sensing. Curr. Biol. *18*, 1587–1593.